A Pontryagin-based NMPC approach for autonomous rendez-vous proximity operations

A Pontryagin-based NMPC approach for autonomous rendez-vous proximity operations

Michele Pagone
Department of Electronics and Telecommunications
Politecnico di Torino
Corso Duca degli Abruzzi, 24, 10129 Torino, Italy
michele.pagone@polito.it

Mattia Boggio
Department of Electronics and Telecommunications
Politecnico di Torino
Corso Duca degli Abruzzi, 24, 10129 Torino, Italy
mattia.boggio@polito.it

Carlo Novara
Department of Electronics and Telecommunications
Politecnico di Torino
Corso Duca degli Abruzzi, 24, 10129 Torino, Italy
carlo.novara@polito.it

Simone Vidano
Department of Electronics and Telecommunications
Politecnico di Torino
Corso Duca degli Abruzzi, 24, 10129 Torino, Italy
simone.vidano@polito.it

Abstract—**This paper proposes a Pontryagin-based approach to Nonlinear Model Predictive Control for autonomous guidance and control in spacecraft maneuvering. The proposed approach guarantees, under suitable conditions, an explicit control law also in presence of nonlinearities. Taking advantage of the Pontryagin Minimum (or Maximum) Principle, the optimization problem solution turns into a two-points boundary value problem, whose differential equations and boundary conditions are the Karush-Kuhn-Tucker necessary conditions of optimality. Conversely to the numerical methods for nonlinear/non-convex optimization, the proposed methodology returns an explicit control law without any a-priori assumption about the input signal parametrization, achieving high performances without increasing the computational complexity of the algorithm. The proposed control algorithm is designed for the proximity operations of a rendez-vous problem which dynamics is described by the so-called Clohessy-Wiltshire equations. A modified NMPC cost function is employed in order to promote the bang-bang behavior of the input signal. This latter yields an improvement of the performances in terms of propellant consumption with respect to the classic quadratic cost indexes.**

TABLE OF CONTENTS

1. INTRODUCTION 1
2. SPACECRAFT LINEARIZED DYNAMICS 2
3. NONLINEAR MODEL PREDICTIVE CONTROL SETTING 2
4. NONLINEAR MODEL PREDICTIVE CONTROL EXPLICIT SOLUTION 3
5. THE RENDEZ-VOUS PROBLEM 4
6. SIMULATED EXAMPLE 5
7. CONCLUSION 7
REFERENCES 7
BIOGRAPHY 8

1. INTRODUCTION

Since the dawn of space exploration, the rendez-vous (RdV) and docking maneuvers - between a chaser and a target - represent some of the most critical in-orbit operations. The maneuver consists in guiding and controlling a chaser spacecraft (S/C) so that it achieves the same orbit of a target satellite in order to approach it at a very close distance (see, e.g. [1]). The first successful attempt was carried out during the Gemini 8 mission, when a manned spacecraft docked an unmanned target in Low-Earth Orbit (LEO). The mission was designed for testing the complex RdV maneuver which would have taken place in Lunar orbit during the Apollo Moon's exploration missions. With the coming of the LEO space stations (e.g. Saljiut, Skylab, Mir, ISS, Tiangong), the RdV and docking operations assumed a fundamental role due to the need of supplying the space stations with the fundamental resources for supporting the astronauts' in-orbit life, as well as to guarantee a continuous turnover of the crew (see, e.g., [2] and [3]). Furthermore, in recent years, the RdV operations have been catching more attention among the space research in the framework of multi-purpose space servicing vehicles for in-orbit servicing and/or active debris removal. These kinds of S/Cs must guarantee a high technological standard to autonomously perform complex tasks in space (e.g. refuelling service [4], small in-orbit reparations, debris removal [5], non-collaborative target capture [6][7]).

In this context, the autonomous guidance and control strategies are becoming key elements in space industry and research, since they allow to optimize the resources expenditure in designing space missions and to extend the spacecraft lifetime by reducing the propellant consumption (see, e.g., [8] and [9]). The Model Predictive Control (MPC) plays a key role within the space control environment, owning a great potential for wide applications in future space missions - which often involve strong nonlinear dynamics - thanks to its capability to deal with Multi-Input Multi-Output (MIMO) systems, input and state constraints and to optimize different kinds of performance indexes. Furthermore, the main MPC advantage is the capability to efficiently join the guidance and control tasks into a single algorithm, designing a probe able to autonomously plan the required maneuvers with a strongly reduced human effort. Examples of MPC applications for RdV and proximity maneuvers include [10], [11], which tackles the RdV problem in the context of the restricted three-body problem, [12], which proposes a sum-of-norms minimum fuel controller, and [13], which achieves the sparsity in solution by employing a LASSO MPC.

This paper presents a novel nonlinear MPC (NMPC) framework for autonomous guidance and control during the rendezvous proximity maneuver between a chaser S/C and a generic non-collaborative target (a space station. an end-of-life satellite, a debris, etc.). The NMPC optimization process takes advantage of the Pontryagin Minimum (or Maximum) Principle (PMP), which, under suitable conditions, provides an explicit control law, also in presence of nonlinearities [14]. This latter is a fundamental point, since, when dealing with a nonlinear optimization problem, the explicit solution is rarely

available. Indeed, starting from the dual formulation of the optimal control problem (OCP), the Hamiltonian scalar function and the Lagrange (or co-state) variables are introduced, such that the OCP is transformed into a standard Two-Points Boundary Value Problem (TPBVP), which solution provides the gains for the explicit optimal control law. The advantages of the proposed methodology are the following: i) the gradient of the Hamiltonian with respect to the input vector provides an efficient explicit strategy for the optimal guidance, whereas it is not available with the primal OCP solution; ii) input and (nonlinear) state constraints are incorporated within OCP with slight modifications of the algorithm by means of the barrier functions method (see, e.g., [15]); iii) since the guidance and the control law are available in an explicit form, the tuning of the NMPC design parameters requires a minor effort. The proposed NMPC algorithm is designed for the RdV problem, which dynamics is described by the Clohessy-Wiltshire equations [16]. In our work we employ a minimum-fuel cost function, promoting the bang-bang behavior of the controller and leading to a sparse-in-time input profile. These features yield improvements in terms of propellant consumption with respect to the classic quadratic performance indexes.

The paper is organized as follows: in Section 2 we describe the S/C motion during the RdV proximity operations. In Section 3 we introduce the NMPC mathematical formulation, its explicit solution is dealt in Section 4 and, afterwards, is tailored for the RdV problem in Section 5. The simulated example is shown in Section 6. Finally, the conclusion are drawn in Section 7.

2. SPACECRAFT LINEARIZED DYNAMICS

In most of aerospace applications, the S/C motion can be described by means of an affine-in-the-input nonlinear system:

$$\dot{x}(t) = f(x(t)) + g(x(t))u(t) \tag{1}$$

where $x \in \mathbb{R}^{n_x}$, $u \in \mathbb{R}^{n_u}$ are the state and the input respectively, and implicitly assuming that the state x coincides with the output. Examples include the two-body dynamics, which can be equally described with the position/velocity equations [16] and/or the Gaussian variational formulation of the Keplerian orbital elements [16] or the equinoctial orbital elements [17].

When dealing with the relative motion for orbit phasing, RdV, and docking operations, different alternative models of S/C motions are available (see [18] and the references therein), commonly based on the approximation/linearization of two-body equations (see, e.g. [19]). In this paper we exploit the so called Clohessy-Whiltshire (C-W) equations. The C-W equations describe the relative motion between a chaser spacecraft and a target. The relative dynamics is based on the linearization of the Keplerian S/C dynamics when (i) the chaser and the target lies on near-circular orbits; (ii) the chaser-target distance is much shorter than the geocentric distance; (iii) the orbital perturbations are neglected. In formulae:

$$\begin{aligned} \ddot{r}_x &= 3\varpi^2 r_x + 2\varpi \dot{r}_y + u_x \\ \ddot{r}_y &= -2\varpi \dot{r}_x + u_y \\ \ddot{r}_z &= -\varpi^2 r_z + u_z \end{aligned} \tag{2}$$

where $r = (r_x, r_y, r_z)^T$ is the chaser position, $\varpi = \sqrt{\mu/a^3}$ is the mean motion, a is the radius of the target's circular orbit (which coincides with the semi-major axis), and μ is the standard gravitational parameter. The state is $x = (r_x, r_y, r_z, \dot{r}_x, \dot{r}_y, \dot{r}_z)^T$ and the input is $u = (u_x, u_y, u_z)^T$.

The orbital reference frame is defined as follows: the origin is located in the target's center of mass, the x-axis (commonly named R-bar) lies along the vector joining the target with the Earth's center, the y axis (H-bar) points in the opposite direction of the orbit normal, and the z-axis (V-bar) is measured positive in the direction of orbital motion, according to a right-handed reference frame. Note that, in (2), the relative motion can be decoupled in the in-plane motion (x-y plane) and the out-of-plane motion (z direction).

3. NONLINEAR MODEL PREDICTIVE CONTROL SETTING

Consider the system in (1), we assume that the state is measured on-line, with a sampling time T_s. If this assumption does not hold, an observer must be employed. The measurements are $x(t_k),\ t_k = T_S k, k = 0, 1, \ldots$. At each time $t = t_k$, a prediction of the system state over the interval $[t, t+T_p]$ is performed, where $T_p > T_s$ is the prediction horizon. The prediction is obtained by the integration of (1). At any time $\tau \in [t, t+T_p]$, the predicted state $\hat{x}(\tau) \equiv \hat{x}(\tau, u(t:\tau))$ is a function of the 'initial' state $x(t)$ and the input signal $u(t:\tau)$. Note that, the notation $u(t:\tau)$ is used to indicate a signal in the interval $[t, \tau]$. Note also that, over the prediction horizon inverval $[t_k, t_k+T_p]$, we can alternatively denote the initial time instant with $t_0 \equiv t_k$ and the final time instant with $t_F \equiv t_k + T_p$.

At each time $t = t_k$, we look for an optimal input signal $u^*(t : t+T_p)$, minimizing a suitable cost function $J(u(t : t+T_p))$, subject to possible constraints that may occur during the system's operations. Mathematically, at each time $t = t_k$ the following optimization problem is solved:

$$\begin{aligned} &u^*(t : t+T_p) = \arg\min_{u(\cdot)} J(u(t : t+T_p)) \\ &\text{subject to:} \\ &\dot{\hat{x}}(\tau) = f(\hat{x}(\tau)) + g(x(\tau))u(\tau),\ \ \hat{x}(t) = x(t) \\ &\hat{x}(\tau) \in X_C,\ u(\tau) \in U_C. \end{aligned} \tag{3}$$

X_C and U_C are sets describing possible constraints on the state and input, respectively. A receding control horizon strategy is employed: at a given time $t = t_k$, only the first optimal input is applied to the plant, the remainder of the solution is discarded. Then, the complete procedure is repeated at the next time $t = t_{k+1}$.

Remark. The optimization problem (3) is numerically not tractable, since $u(\cdot)$ is a continuous-time signal and then the number of decision variables is potentially infinite. To overcome this issue, when the optimum is found numerically, an a-priori finite parametrization of the input signal $u(\cdot)$ must be assumed. For example, a piece-wise constant parametrization can be assumed, with changes of value at the nodes $\tau_1, \ldots, \tau_{n_N} \in [t, t+T_p]$. Note that, as it will be dealt in Section 4, the PMP-based NMPC solution does not require any a-priori assumption about the control signal parametrization.

4. NONLINEAR MODEL PREDICTIVE CONTROL EXPLICIT SOLUTION

According to [20], the functional J can be taken as a sum of weighted signal and vectors norms. We recall the definition of the $\mathscr{L}_p$ signal norm in continuous time:

$$\mathscr{L}_p = \left(\int_I \|f(t)\|_q^p \, \mathrm{dt} \right)^{1/\mathrm{p}} \tag{4}$$

where $||\cdot||_q$ is a vector norm with $q \geq 1$. Since the goal of the optimization problem is to minimize the propellant consumption during the RdV maneuver, as suggested by [12] and [21], we minimize the $\mathscr{L}_1$ of the input, since it effectively leads to a minimum-propellant controller design. To sum up, we employ the following mixed $\mathscr{L}_1/\mathscr{L}_2^2$ functional:

$$\begin{aligned} J = \int_t^{t+T_P} \|\tilde{x}_p(\tau)\|_Q^2 + \|\mathbf{R}u(\tau)\|_q \, \mathrm{d}\tau \\ + \|\tilde{x}_p(t+T_P)\|_P^2. \end{aligned} \tag{5}$$

The $\|v\|_W^2$ notation represents the (square) weighted norm of a vector $v \in \mathbb{R}^n$ such that $\|v\|_W^2 \doteq v^T W v \doteq \sum_{i=1}^n w_i v_i^2$ and $W = \mathrm{diag}(w_1, ..., w_n) \in \mathbb{R}^n$, $w_i \geq 0$. The predicted tracking error is $\tilde{x}_p(\tau) = r(\tau) - \hat{x}(\tau)$, whereas $r(\tau)$ is the desired reference to track and $\hat{x}(\tau)$ is obtained by integration of (1). The weights $\mathbf{Q} \geq 0$, $\mathbf{R} > 0$ and $\mathbf{P} \geq 0$ are diagonal matrices. Note that, $\mathbf{Q}, \mathbf{P} \in \mathbb{R}^{n_x \times n_x}$ and $\mathbf{R} \in \mathbb{R}^{n_u \times n_u}$.

Recalling the (3), we define the U_C and X_C sets describing possible constraints affecting the input and the state respectively. In the case of state constraints, we define the nonlinear set as $X_C = \{x(t) \in \mathbb{R}^{n_x} : C(x(t)) \leq 0, \forall t\}$, whereas $C(x(t))$ is a nonlinear function depending both from state and time. As for the input constraints, the control signal is bounded into the set $U_C = \{u(t) \in \mathbb{R}^{n_u} : \|u(t)\|_q \leq u_{max}, \forall t\}$.

Pontryagin-based Optimization Algorithm

According to [14], the necessary condition for a control $u(t)$ to be optimal and a trajectory $x(t)$ to be the extremal path is that the Hamiltonian scalar function $H(x(t), u(t), \lambda(t))$ attains its minimum value when $u(t) = u^*(t)$. Keeping implicit the time dependence, the Hamiltonian function is defined as:

$$H(x, u, \lambda) = \Phi(x, u) + \lambda^T \big(f(x) + g(x)u\big) \tag{6}$$

where λ is the vector of Lagrangian (or co-state) variables and $\Phi(x,u)$ is the integrand function in (5), i.e. $\Phi(x,u) = \|\tilde{x}_p\|_Q^2 + \|\mathbf{R}u\|_q$. The optimization problem is subject to both the dynamics in (1) and the dynamics of the co-state variables $\dot{\lambda}$, which evolution is described by the so-called Euler-Lagrange differential equations:

$$\dot{\lambda} = -\nabla_x \big(H(x, u, \lambda)\big) \tag{7}$$

where $\nabla_z(\cdot)$ notation depicts the gradient operator with respect to the generic vector variable z. The state and co-state dynamics are the first-order optimality conditions. These latter differential equations must satisfy a set of boundary conditions to be imposed, at the borders of the prediction horizon, both on the state and the co-state. As for the state, at each time $t = t_k$ the value cannot be chosen arbitrarily: the continuity between two successive sampling steps must be ensured, whereas the same continuity condition is no required for the co-states. On the other hand, the λ vector must satisfy the boundary conditions for optimality (see [22]) at the end of prediction horizon. In formulae:

$$\begin{aligned} x_0 &= x(t_0) \\ \lambda(t_F) &= \nabla_{x(t_F)} \phi(x(t_F)) \end{aligned} \tag{8}$$

where $\phi(x(t_F))$ is terminal cost rate of the functional, i.e. $\phi(x(t_F)) = \|\tilde{x}_p(t+T_P)\|_P^2$.

Therefore, according to the PMP, the optimal control satisfies

$$u^*(t) = \arg\min_{u(\cdot)} H(x, u, \lambda), \tag{9}$$

which is equivalent to solve the equation

$$\nabla_{u(\cdot)} H(x, u, \lambda) = 0. \tag{10}$$

In the case of affine-in-the-input systems, the solution of (9), over the prediction horizon, is quite trivial and has the following general form:

$$u^*(\tau) = -\mathbf{R}^{-1} \lambda(\tau)^T g(x(\tau)) \tag{11}$$

where $\mathbf{R}$ is the diagonal, constant, square and full rank matrix introduced in (5). Since the receding control horizon strategy is adopted, only the first sample of $u^*(\tau)$ is applied to the plant and the remainder of the solution is discarded.

In summary, the (1) jointly with the (7) and the boundary conditions in (8) represent a TPBVP to be solved over the prediction horizon $[t, t+T_p]$. The TPBVP solution provides the λ (i.e. the gains) of the explicit control law (11), hence, turning the OCP into a standard TPBVP. Note that, (1), (7), and (8) are the Karush-Kuhn-Tucker (KKT) conditions of the dual optimization problem (see, e.g. [23]).

Remark. According to the PMP, the Hamiltonian minimization provides a local minimum for the the nonlinear optimization problem, i.e. a sub-optimal solution. However, also numerical methods (e.g. sequential quadratic programming) would have returned a local minimum. Therefore, a PMP sub-optimal solution is not an issue when dealing with non-convex/nonlinear optimization problems.

Remark. The (10) - together with the KKT conditions - provides the first-order necessary requirement for a local minimum. Nevertheless, a sufficient condition is given when $\partial^2 H / \partial u^2 \geq 0$ (Legende-Clebsch condition), the normality condition, and the Jacobi condition are verified (for further details, see [22] and [24]).

Remark. As already mentioned in Section 3, the Pontryagin-based NMPC solution does not require an a-priori parametrization of the input signal $u(t)$. Indeed, as highlighted in (11), the optimal control $u^*(\tau)$ depends on $\lambda(\tau)$ which varies, according to the Euler-Lagrange equation (7), over the whole prediction horizon. This is a very interesting result since the OCP algorithm achieves high performances without increasing the computational complexity and without any a-priori assumption on the input signal shape.

Path Constraints Management

A way to incorporate the path constraints within the OCP is to define an augmented cost function $\tilde{J}$ such that, when the state trajectory approaches the boundary of the forbidden

set, its value tends to infinity: $\lim_{C(x)\to 0}\tilde{J}=\infty$. Thanks to this strategy, the constrained OCP is solved with the same procedure described in the previous section. Hence, we augment the cost function with a suitable barrier function $k(x)$ which prevents the trajectory to approach the boundaries of the forbidden sets whilst its value is (almost) null when far from the boundaries. This is a common methodology for dealing with path constraints, examples are included in [25]. Thus, the cost function turns into:

$$\begin{aligned}\tilde{J}=\int_t^{t+T_P}\|\tilde{x}_p(\tau)\|_Q^2+\|\mathbf{R}u(\tau)\|_q+\sum_{i=1}^n k_i(x)\,\mathrm{d}\tau\\ +\|\tilde{x}_p(t+T_P)\|_P^2.\end{aligned}\tag{12}$$

where n is the number of the state constraints. Given the augmented performance index $\tilde{J}$, the solution of the TPBVP follows the same aforementioned procedure, accounting the gradient of the barrier function within the Euler-Lagrange differential equations.

5. The Rendez-vous Problem

Once that the complete NMPC solution procedure has been presented, the OCP can be further detailed by integrating the RdV satellite motion. Let the path constraints be momentarily neglected. In our specific problem, we chose not to consider the S/C mass variation due to the maneuvers. This is a common choice if considering electric propulsion with very high values of specific impulse (I_{sp}). If the $I_{sp}\sim 1000\ s$ (or higher), the amount of propellant burned during the maneuvers is a very small fraction of the overall satellite mass which, without loss of generality, can be considered constant throughout the whole approaching phase.

Accounting the C-W relative motion equations (2) and the performance index (5) (setting $q=2$), the Hamiltonian turns into (keeping implicit the time dependence):

$$\begin{aligned}H(x,u,\lambda)=\|\mathbf{R}u\|_2+\tilde{x}_p^T\mathbf{Q}\tilde{x}_p+\lambda_x\dot{r}_x+\lambda_y\dot{r}_y+\lambda_z\dot{r}_z\\ +\lambda_{\dot{x}}(3\varpi^2 r_x+2\varpi\dot{r}_y+u_x)+\lambda_{\dot{y}}(-2\varpi\dot{r}_x+u_y)\\ +\lambda_{\dot{z}}(-\varpi^2 r_z+u_z)\end{aligned}\tag{13}$$

where $\lambda=(\lambda_x,\lambda_y,\lambda_z,\lambda_{\dot{x}},\lambda_{\dot{y}},\lambda_{\dot{z}})^T$ is the co-state vector. Whereby, the Euler-Lagrange equations in compact form:

$$\dot{\lambda}=\mathbf{A}\lambda-2\mathbf{Q}\tilde{x}\,,\tag{14}$$

$$\mathbf{A}=\begin{bmatrix}\mathbf{0}_{3\times 3} & \mathbf{W}\\ -\mathbf{I}_{3\times 3} & \mathbf{M}\end{bmatrix},\tag{15}$$

$$\mathbf{W}=\begin{bmatrix}-3\varpi^2 & 0 & 0\\ 0 & 0 & 0\\ 0 & 0 & \varpi^2\end{bmatrix},\ \mathbf{M}=\begin{bmatrix}0 & 2\varpi & 0\\ -2\varpi & 0 & 0\\ 0 & 0 & 0\end{bmatrix},\tag{16}$$

and $\mathbf{I}$ is the identity matrix. The boundary conditions on λ are imposed at the end of the prediction horizon while the continuity of the state must be imposed at the beginning of the prediction horizon, from (8) we have:

$$\begin{aligned}x_0=x(t_0)\,,\\ \lambda(t_F)=2\mathbf{P}\tilde{x}_p(t_F).\end{aligned}\tag{17}$$

We have formalized the TPBVP for the RdV dynamics. The solution of TPBVP provides the values of λ of the explicit control law. As already mentioned, the minimization of the $\mathscr{L}_1$ norm of the input signal promotes the bang-bang behavior of the controller, this latter happens when the input signal appears linearly in the Hamiltonian.

Definition 1: A controller is said 'bang-bang' when its output can only assume a null, a maximum or a minimum value. The resulting command signal is piece-wise constant in time.

In order to explicit the optimal control law for the RdV problem, let the Hamiltonian be slightly modified. Define with Γ the magnitude of the thrust acceleration, such that $\Gamma=\|u\|_2$, and $\hat{u}$ is the thrust acceleration unit vector. Subdivide also the co-state vector into two smaller vectors $\lambda_R=(\lambda_x,\lambda_y,\lambda_z)^T$ and $\lambda_V=(\lambda_{\dot{x}},\lambda_{\dot{y}},\lambda_{\dot{z}})^T$. The Hamiltonian is re-written as:

$$H=\|\mathbf{R}u\|_2+\tilde{x}_p^T\mathbf{Q}\tilde{x}_p+\lambda_R^T v+\lambda_V^T(h(x)+\Gamma\hat{u})\tag{18}$$

where $v=(\dot{r}_x,\dot{r}_y,\dot{r}_z)^T$ is the velocity vector and $h(x)=(3\varpi^2 r_x+2\varpi\dot{r}_y,-2\varpi\dot{r}_x,-\varpi^2 r_z)^T$. Consider the cost rate $\|\mathbf{R}u\|_2$, it is well know that $\|\mathbf{R}u\|_2\le\|\mathbf{R}\|_2\|u\|_2$, nevertheless, if $\mathbf{R}$ is a definite positive diagonal matrix whose entries are all equal, the $\|\mathbf{R}u\|_2=\|\mathbf{R}\|_2\|u\|_2$ equality holds. This latter assumption is quite common in aerospace fields, where the weights relevant to thrust acceleration components are all equal. Therefore, the (18) turns into:

$$H=\|\mathbf{R}\|_2\Gamma+\tilde{x}_p^T\mathbf{Q}\tilde{x}_p+\lambda_R^T v+\lambda_V^T(g(x)+\Gamma\hat{u}).\tag{19}$$

We take now advantage of the notion of primer vector p, a remarkable property of the Lagrangian variables provided by Lawden in [26]. Indeed, the vector of the Lagrangians associated to the velocity λ_V represents the optimal firing direction and its well know in literature as 'primer vector', so that $p=-\lambda_V$. Therefore, the optimal thrust direction is parallel to the primer vector direction and then $\hat{u}=p/P$, being $P=\|p\|_2=\|-\lambda_V\|_2$ the primer vector magnitude. Hence, $P=-\lambda_V^T\hat{u}$. By the previous definitions, the Hamiltonian is re-written as:

$$\begin{aligned}H&=\|\mathbf{R}\|_2\Gamma+\tilde{x}_p^T\mathbf{Q}\tilde{x}_p+\lambda_R^T v+\lambda_V^T g(x)-P\Gamma\\ &=-(P-\|\mathbf{R}\|_2)\Gamma+\tilde{x}_p^T\mathbf{Q}\tilde{x}_p+\lambda_R^T v+\lambda_V^T g(x).\end{aligned}\tag{20}$$

According to (9), the Hamiltonian must be minimized over the choice of the thrust acceleration magnitude Γ. Nevertheless, since the acceleration appears linearly in the Hamiltonian, the solution of the optimal control equation will lead to an input signal with an infinite magnitude. In this peculiar case, the problem is feasible if and only if the control is bounded. If the control belongs to a bounded set, the minimizing value of the Hamiltonian will depend only on the algebraic sign of the coefficient of Γ in (20). In the aerospace literature, the coefficient of the thrust magnitude is well known as switching function (SF). In this particular case, it is defined as:

$$SF=P-\|\mathbf{R}\|_2.\tag{21}$$

The sign of the switching function defines a policy for the engines power-on/off. Therefore, the solution that minimizes the Hamiltonian function is bang-bang control law and the input signal can assume only a maximum or zero value:

$$\Gamma=\begin{cases}\Gamma_{max} & \text{if}\quad \mathrm{SF}>0,\\ 0 & \text{if}\quad \mathrm{SF}<0.\end{cases}\tag{22}$$

Table 1. **Orbital Scenario Parameters**

Description	Value	Unit
Earth's Planetary. Const. (μ)	398600.4418	$\mathrm{km}^3\,\mathrm{s}^{-2}$
Earth's Gravity Acc.(g_0)	9.807	$\mathrm{km}\,\mathrm{s}^{-2}$
Orbit Radius	42164	km
Mean Motion (ϖ)	7.2911e-05	s^{-1}

When $SF = 0$, the control is called singular (or undetermined) and it can assume any value into the admissible input set. Clearly, when the control is singular, a suitable choice is to set $\Gamma = 0$.

To sum up, we have defined a policy for the engines ignition and we have proved that the $\mathscr{L}_1$ minimization of the input signal provides a bang-bang control law, which magnitude can assume only the zero or the maximum values. As for the firing direction, we remind that the optimal thrust direction is parallel to the primer vector direction. Briefly, the optimal control law assumes the final form:

$$u^* = \begin{cases} \Gamma_{max} \dfrac{p}{\|\lambda_V\|_2} & \text{if} \quad \text{SF} > 0, \\ 0 & \text{if} \quad \text{SF} \leq 0. \end{cases} \tag{23}$$

Note that, when minimizing with respect to the Euclidean norm of the input, the bang-bang behavior refers to the magnitude of thrust whilst the single components can assume any value according to (23). Conversely, if we would have been minimized with respect to the $\|\cdot\|_1$ of the input signal, the bang-bang behavior would have been appeared element-wise.

6. SIMULATED EXAMPLE

Consider a scenario where the chaser satellite is approaching the target starting from a distance of few hundreds meters, in order to allow the subsequent docking maneuver. The dynamics is described by the C-W equations in (2) and the operations take place in a geostationary orbit. The orbital scenario parameters are summarized in Table 1. The trajectory of the chaser is subject to nonlinear constraints. In the example scenario, we design a safety sphere around the target (in order to avoid possible chaser/target collisions) with a radius of 0.05 *km*. Therefore, the admissible state set is defined as:

$$X_C = \left\{ x(t) \in \mathbb{R}^6 : 0.05 - \|r(t)\|_2 \leq 0, \forall t \right\} \tag{24}$$

The path constraint is handled by designing a proper barrier function which prevents the S/C to violate the safety sphere around the target. We chose to employ a Gaussian-like barrier function of the form:

$$k(x) = a \exp\left(-bC(x)^2\right) \tag{25}$$

where a and b are shaping parameters to be tuned during the design phase and $C(x) \equiv 0.05 - \|r(t)\|_2$. Conversely to other kinds of barrier functions (e.g. the log-like functions), when $C(x) \to 0$, the value of $k(x)$ is very high without reaching the infinity. This choice prevents several numerical errors that may occur when the S/C is too close to the safety sphere. In order to include the barrier function within the Euler-Lagrange equation, we explicit the gradient of $k(x)$ with respect to state x:

$$\nabla_x k(x) = \begin{bmatrix} -2abr_x \exp\left[-b(\|r\|_2 - 0.05)^2\right] \dfrac{\|r\|_2 - 0.05}{\|r\|_2} \\ -2abr_y \exp\left[-b(\|r\|_2 - 0.05)^2\right] \dfrac{\|r\|_2 - 0.05}{\|r\|_2} \\ -2abr_z \exp\left[-b(\|r\|_2 - 0.05)^2\right] \dfrac{\|r\|_2 - 0.05}{\|r\|_2} \\ 0 \\ 0 \\ 0 \end{bmatrix} \tag{26}$$

Table 2. **S/C Parameters**

Description	Symbol	Value
Mass	m	$500\ kg$
Init. Position	r_0	$(-0.5, -0.1, 0.3)^T\ km$
Init. Velocity	$\dot{r}_0$	$(-0.001, -0.008, -0.001)^T\ km/s$
Ref. Position	r_r	$(0.08, 0, 0)^T\ km$
Ref. Velocity	$\dot{r}_r$	$(-0.001, 0, 0)^T\ km/s$

Table 3. **Engine Parameters**

Description	Symbol	Value
Specific Impulse	I_{sp}	$1800\ s$
Maximum Thrust	T_{max}	$0.49\ N$
Maximum Acceleration	u_{max}	$5e-5\ km/s^2$

Let now the S/C dynamics, the propulsion system, and the NMPC parameters be presented. The initial and the reference state of the chaser S/C are listed in the Table 2. We chose to guide the chaser in order to nullify the y and z components and allowing the target to be approached and docked, in the very last meters of the maneuvers, along the x-axis. Concerning the propulsion system, the S/C is equipped with a cluster of electric engines whose main parameters are highlighted in Table 3. This choice is aimed to promote the propellant expenditure minimization, allowing the S/C to extend its mission life time and to equip heavier payloads. Finally, the NMPC design parameters are listed in Table 4.

Table 4. **NMPC Parameters**

Parameter	Value
T_S	$1\ s$
T_p	$60\ s$
$\mathbf{R}$	$\mathbf{I}_{3\times3}$
$\mathbf{Q}$	$20 \cdot \mathbf{I}_{3\times3}$
$\mathbf{P}$	$diag(10, 10, 10, 1, 1, 1)$
a	1000
b	1000

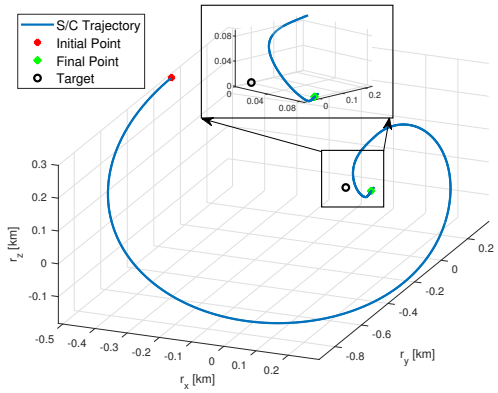

Figure 1. Chaser Trajectory.

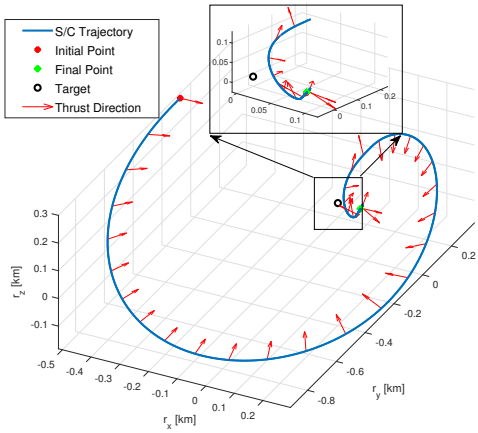

Figure 2. Chaser Trajectory and Thrust Direction.

We are now in position to present the outcomes of the simulations. The orbital simulator and the NMPC algorithm are implemented in the Matlab/Simulink environment. In Figure 1, the chaser trajectory is sketched, showing the motion of the S/C from the initial point towards the reference point. Moreover, in Figure 2, the thrust direction is shown along the S/C trajectory. Nevertheless, Figure 3 and Figure 4 give more worthy information about the trajectory evolution of the S/C during the maneuver. Indeed, from Figure 3, it is possible to observe how the guidance and control algorithm is perfectly able to track the desired reference position. On the other hand, the chaser position radius (Figure 4) shows how the S/C never violates the safety sphere around the target. This is also due to the large value of the $\mathbf{Q}$ which allows to smooth the oscillatory evolution of the state.

As for the S/C velocity, the evolution is shown in Figure 5. A very important point: since during the approaching phase the requirement on the reference velocity is not so strict (as it will happen in the docking phase), the tolerance on the reference has been relaxed. This latter helps to reduce the computational effort and the time of the maneuver.

An interesting discussion can be carried out by analyzing the plot of the thrust components and magnitude. As already mentioned in Section 5, we designed a NMPC cost index in order to obtain a bang-bang profile of the input. This behavior is clear by observing the thrust acceleration magnitude in the last subplot of Figure 6. Indeed, we remind that the bang-

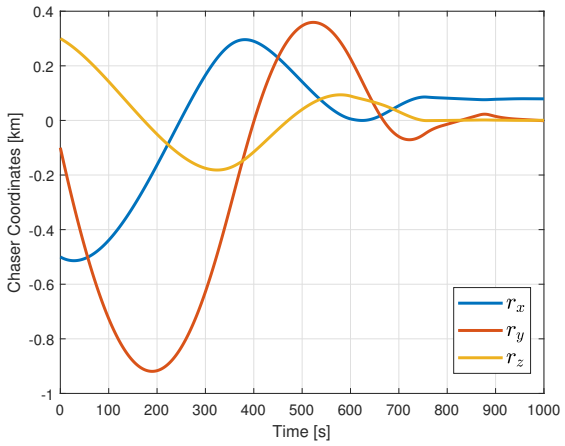

Figure 3. Chaser Position Coordinates.

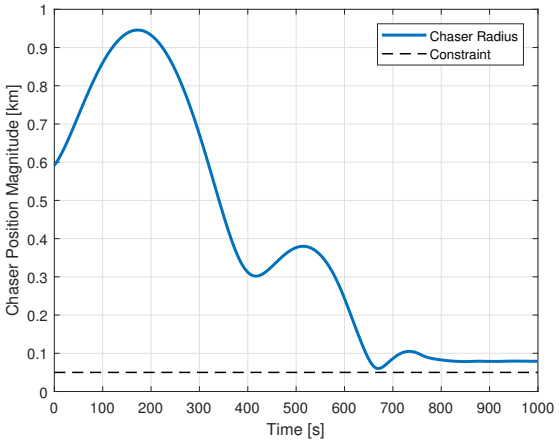

Figure 4. Chaser Position Magnitude.

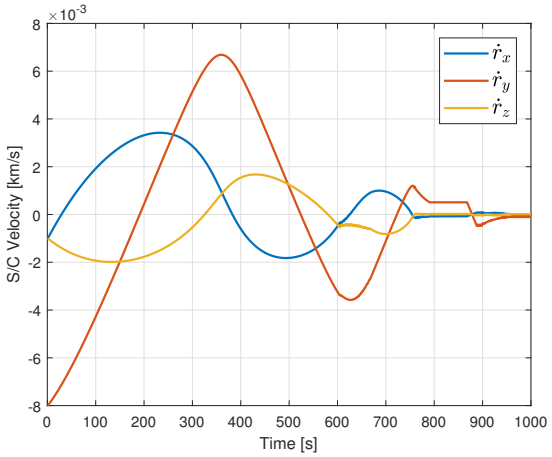

Figure 5. Chaser Velocity Components.

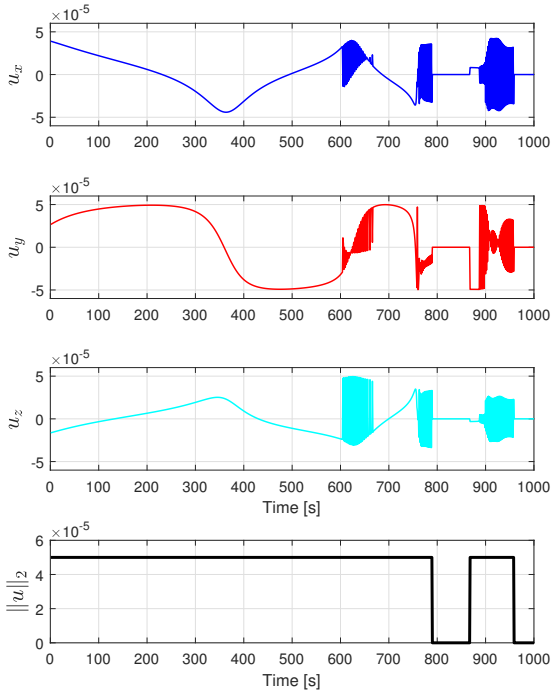

Figure 6. Thrust Components and Magnitude.

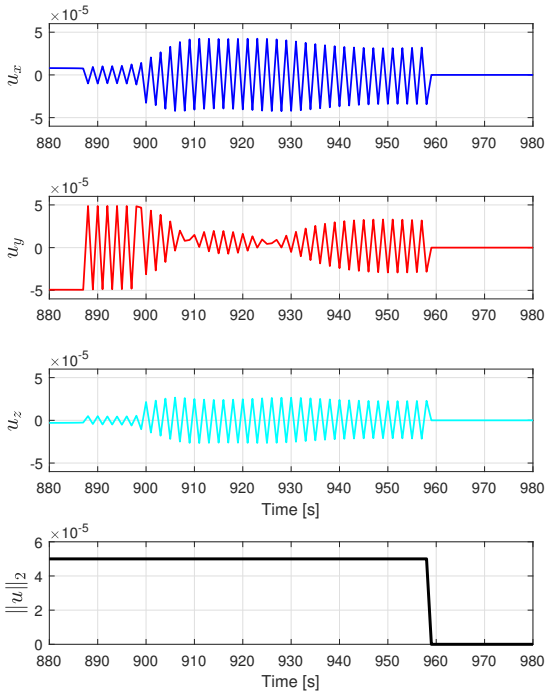

Figure 7. Zoom of Thrust Components and Magnitude.

bang behavior is meant referred to the magnitude acceleration and not component-wise. For this reason, the single components of the thrust can assume any value within the input set, being the input constraints always satisfied. In Figure 7, the thrusting acceleration components and magnitude are displayed for the last phase of the RdV maneuver. Even though the thrust acceleration evolution presents a high-frequency behavior, the issue can be mitigated through a proper control dispatch during the S/C engines configuration design. Finally, concerning the mass (Figure 8), it can be observed that, during the maneuver, only a very small fraction of the overall S/C mass is burned (about 1.2 kg). Therefore, without loss of generality, we can considered the S/C to have a constant mass throughout all the maneuver interval.

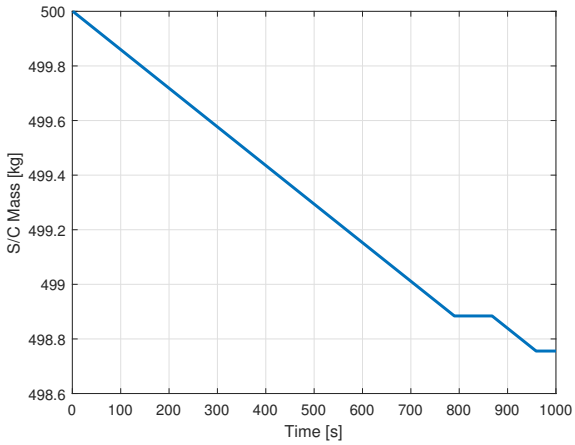

Figure 8. Mass Variation.

7. Conclusion

The problem of obtaining an explicit control law for the Nonlinear Model predictive Control was studied. We have developed an algorithm that, thanks to the Pontryagin Minimum Principle, was able to switch from the primal optimization problem to the dual formulation. This approach guarantees the availability of an explicit control law which is function of the co-state variables, whose evolution is described by the Euler-Lagrange equations. Indeed the optimal solution was obtained by minimizing the Hamiltonian scalar functions, an operation that can be tackled analytically by solving an algebraic equation. Moreover, the integration of the path constraints was managed by exploiting a suitable barrier function, with a slight modification of the NMPC cost function, and without any modification of the OCP algorithm. Another key point of the dissertation was the employment of a mixed $\mathscr{L}_1/\mathscr{L}_2^2$ functional, which yielded a sparse-in-time and bang-bang behavior of the solution. The novel approach was applied to a rendezvous space mission, which dynamics is described by Clohessy-Wiltshire equations. The chaser is equipped with low-thrust engines and a safety sphere around the target was designed in order to avoid possible chaser/target collisions. The result highlighted the effectiveness of the NMPC algorithm, showing an excellent reference tracking, the compliance with the path constraints, and the desired bang-bang behavior of the engines.

References

[1] H.B. Hablani, M.L. Tapper, D.J. Dana-Bashian, Guidance and Relative Navigation for Autonomous Ren-

dezvous in a Circular Orbit, Journal of Guidance, Control, and Dynamics, Vol. 25, No. 3, May-June 2002.

[2] J. Fabrega, M. Frezet, J.L. Gonnaud, ATV GNC during rendezvous, Spacecraft Guidance, Navigation and Control Systems, 381, 85-93, 1997.

[3] P. Miotto, L. Breger, I. Mitchell, B. Keller, B. Rishikof, Designing and Validating Proximity Operations Rendezvous and Approach Trajectories for the Cygnus Mission, Proceedinds of the AIAA Guidance, Navigation, and Control Conference, Toronto, Canada, 2-5 August 2010.

[4] A. Medina, A. Tommasini, M. Suatoni, M. Avilés, et alii, Towards a Standardized Grasping and Refuelling On-Orbit Servicing for GEO Spacecraft, Acta Astronautica, Vol. 134, pp. 1-10, May 2017.

[5] T. Yamamoto, N. Murakami, Y. Nakajima, K. Yamanaka, Navigation and Trajectory Design for Japanese Active Debris Removal Mission, Proceedings of the 24th Symposium on Space Flight Dynamics, Laurel, Maryland (USA), May 2014.

[6] M. Jankovic, J. Paul, F. Kirchner, GNC architecture for autonomous robotic capture of a non-cooperative target: Preliminary concept design, Advances in Space Research, Vol. 57, Issue 8, pp. 1715-1736, 2016.

[7] S. Matsumoto, S. Jacobsen, S. Dubowsky, Y. Okhami, Approach Planning and Guidance for Uncontrolled Rotating Satellite Capture Considering Collision Avoidance, Proceedings of the 7th International Symposium on Artificial Intelligence, Robotic and Automation in Space, Nara, Japan, 19-23 May 2003.

[8] R. Serra, D. Arzelier, A. Rondepierre, Analytical Solutions for Impulsive Elliptic Out-of-Plane Rendezvous Problem via Primer Vector Theory, IEEE Transaction of Control Systems Technology, Vol. 26, No. 1, pp. 207-221, January 2018.

[9] D. Lee, H. Pernicka, Optimal Control for Proximity Operation and Docking, International Journal of Aeronautical and Space Sciences, Vol. 11, Issue 3, pp. 206-220, September 2010.

[10] E.N. Hartley, A Tutorial on Model Predictive Control for Spacecraft Rendezvous, European Control Conference, 15-17 July 2015.

[11] J.C. Sanchez, F. Gavilan, R. Vazquez, Chance-constrained Model Predictive Control for Near Rectilinear Halo Orbit spacecraft rendezvous, Aerospace Science and Technology, 100 (2020) 105827.

[12] M. Leomanni, G. Bianchini, A. Garulli, A. Giannitrapani, R. Quartullo, Sum-of-norms model predictive control for spacecraft maneuvering, IEEE Control System Letters, Vol. 3, No. 3, July 2019.

[13] E.N. Hartley, M. Gallieri, J.M. Maciejowski, Terminal Spacecraft rendezvous and capture with LASSO model predictive control, International Journal of Control, 86:11, 2014-2113, 2011.

[14] L.S. Pontryagin, V.G. Boltyanskii, R.V. Gamkrelidze, E.F. Mishchenko, The Mathematical Theory of Optimal Processes, Interscience Publisher, John Wiley and Sons, New York, 1962.

[15] Z. Wang, Y. Li, Indirect method for inequality constrained optimal control problems, IFAC PapersOnLine, Vol. 50, Issue 1, pp. 4070-4075, 2017.

[16] E. Canuto, C. Novara, L. Massotti, D. Carlucci, C. Perez Montenegro, Spacecraft dynamics and control: the embedded control approach, Elsevier Aerospace Engineering Series, Oxford, UK, 2019.

[17] E.A. Roth, The Gaussian form of the variation-of-parameter equations formulated in equinoctial elements - Applications: Airdrag and radiation pressure, Acta Astronautica, Vol. 12, Issue 19, pp. 719-730, 1985.

[18] Y. Luo, J. Zhang, G. Tang, Survey of orbital dynamics and control of space rendezvous, Chinese Journal of Aeronautics, (2014), 27(1): 1-11.

[19] M. Leomanni, G. Bianchini, A. Garulli, A. Giannitrapani, State feedback control in equinoctial variables for orbit phasing applications, Journal of Guidance, Control, and Dynamics, Vol. 41, No. 8, pp. 1815-1822, 2018.

[20] A. Bemporad, F. Borelli, M. Morari, Model predictive control based on linear programming - the explicit solution, IEEE Transaction of Automatic Control, Vol.47, No.12, December 2002.

[21] I.M. Ross, How to find minimum-fuel controllers, AIAA Guidance, Navigation, and Control Conference and Exhibit, 15-19 August 2004.

[22] A.E. Bryson, Y. Ho, Applied optimal control: optimization, estimation and control, Taylor & Francis Inc., 1975.

[23] H. Deng, T. Ohtsuka, A parallel Newton-type method for nonlinear model predictive control, Automatica, 109 (2019) 108560.

[24] A.V. Sarychev, Sufficient optimality conditions for Pontryagin extremals, System & Control Letters, Vo. 19, Issue 6, pp. 451-460, 1992.

[25] C. Wang, C. Ma, J. Zhou, A new class of exact penalty functions and penalty algorithms, Journal of Global Optimization, 58:51-73, 2014.

[26] D.F. Lawden, Optimal Trajectories for Space Navigation, Butterworths, 1963.

BIOGRAPHY

Michele Pagone *was born in Bari (Italy) in 1991. He received the bachelor's degree in 2014 and the master's degree in 2016, both in Aerospace/Astronautical Engineering at Politecnico di Torino. Then, in 2018, he started the Ph.D. degree in Electrical, Electronics, and Communications Engineering at Politecnico di Torino. His research fields are related to space flight mechanics, orbital and attitude control systems, optimal control, and nonlinear optimization. He also cooperated with Thales Alenia Space Italy in the frame of the Carrier Module and the Descent Module GNC for the ESA ExoMars mission.*

Mattia Boggio *received the B.Sc. degree in Electronic Engineering in 2016 and the M.Sc. degree in Mechatronic Engineering in July 2019, both at Politecnico di Torino. Currently, he is Ph.D. Student in Electrical, Electronics, and Communications Engineering at Politecnico di Torino. His research fields are related to optimal and predictive control, nonlinear optimization, autonomous guidance, and aerospace/automotive applications. He also cooperates with Thales Alenia Space Italy for the NGGM mission.*

Carlo Novara *received the Laurea degree in Physics from Universitá di Torino (Italy) in 1996 and the PhD degree in Computer and System Engineering from Politecnico di Torino (Italy) in 2002. He held a visiting researcher position at University of California at Berkeley in 2001 and 2004. He is currently an Associate Professor at Politecnico di Torino (Italy). He is the author or co-author of about 140 scientific peer-reviewed publications in international journals and conferences. He has been involved in several national and international projects and in several research contracts in collaboration with Italian and European companies. He is the co-author of several patents in the automotive field. He is a member of the IEEE TC on System Identification and Adaptive Control, of the IFAC TC on Modelling, Identification and Signal Processing, and a founding member of the IEEE-CSS TC on Medical and Healthcare Systems. His research interests include nonlinear and LPV system identification, filtering/estimation, time series prediction, nonlinear control, predictive control, data-driven methods, set membership methods, sparse methods, and automotive, aerospace, biomedical and energy applications.*

Simone Vidano *was born in Italy in 1990. He obtained a Bachelor's degree in Aerospace Engineering in 2013 and a Master's Degree in Mechatronics Engineering in 2016, both at Politecnico di Torino. Being passionate about space exploration, he carried out an internship at Thales Alenia Space and later he began a Ph.D. focused on space control systems at Politecnico di Torino. His research activities are currently dedicated to the control system design for the LISA space mission, in collaboration with the European Space Agency.*